Asian Journal of Chemistry; Vol. 26, No. 6 (2014), 1848-1852

ASIAN JOURNAL OF CHEMISTRY

http://dx.doi.org/10.14233/ajchem.2014.16403

Cyclic Microwave-Assisted Metathetic Synthesis and Spectroscopic Properties of SPION/$SrWO_4$:Er^{3+}, Yb^{3+} Composites

CHANG SUNG LIM

Department of Advanced Materials Science & Engineering, Hanseo University, Seosan 356-706, Republic of Korea

Corresponding author: Tel/Fax: +82 41 6601445; E-mail: cslim@hanseo.ac.kr

Received: 21 September 2013; *Accepted*: 13 February 2014; *Published online*: 10 March 2014; AJC-14914

Er^{3+}/Yb^{3+} co-doped $SrWO_4$($SrWO_4$:Er^{3+}/Yb^{3+}) composites with superparamagnetic iron oxide nanoparticles (SPIONs) were successfully synthesized by a cyclic microwave-assisted metathetic method followed by heat-treatment. The microstructure exhibited well-defined and homogeneous morphology with the $SrWO_4$:Er^{3+}/Yb^{3+} particle size of 1-2 μm and Fe_3O_4 particle size of 0.1-0.5 μm. The Fe_3O_4 particles were self-preferentially crystallized and immobilized on the surface of $SrWO_4$:Er^{3+}/Yb^{3+} particles. The synthesized SPION/$SrWO_4$:Er^{3+}/Yb^{3+} composites were characterized by X-ray diffraction, scanning electron microscopy and energy-dispersive X-ray spectroscopy. Other spectroscopic properties were also examined using photoluminescence emission measurements and Raman spectroscopy.

Keywords: SPIONs, $SrWO_4$:Er^{3+}/Yb^{3+}, Microwave-assisted metathetic synthesis, SEM, EDX, Raman spectroscopy.

INTRODUCTION

Multifunctional nanocomposites that exhibit significant magnetic moment and luminescence have attracted much attention because of various applications in biotechnology, medicine and quality inspection. The superparamagnetic iron oxide nanoparticles (SPIONs) incorporated into photoluminescent composites containing two different functionalities could provide novel characteristics *via* the integration of fluorescent and magnetic properties, offering new potential in a wide range of applications in biomedical systems, such as targeted drugs, diagnostics, therapeutics and bio-imaging[1-3]. The particles of rare-earth-doped upconversion of $SrWO_4$ which shows a Schleelite-type structure with unit cell parameters a = b = 5.417 Å and c = 11.951 Å[4], are relatively stable in the air and have stable physical and chemical properties, low excitation threshold energy and low-cost productivity. Recently, several processes have been developed to increase the applications of rare-earth-doped metal tungstates prepared using a range of processes including solid-state reactions[5,6], the sol-gel method[7], the hydrothermal method[8,9], the combustion method[10], the solvothermal route[11] and the sonochemical method[12]. For practical application of photoluminescence in such products as lasers, three-dimensional displays, light-emitting devices and biological detectors, features such as homogeneous particle size distribution and morphology need to be well defined.

The cyclic microwave-assisted metathetic synthesis of materials is a simple and cost-effective method that provides a high yield with an easy scale-up and it is emerging as a viable alternative approach for the synthesis of high-quality novel inorganic materials in short time periods[13]. In this study, the Er^{3+}/Yb^{3+} co-doped $SrWO_4$ ($SrWO_4$:Er^{3+}/Yb^{3+}) and Er^{3+}/Yb^{3+} co-doped $SrWO_4$ with SPIONs (SPION/$SrWO_4$:Er^{3+}/Yb^{3+}) composites were synthesized by the cyclic microwave-assisted metathetic method followed by heat-treatment. The synthesized $SrWO_4$:Er^{3+}/Yb^{3+} and SPION/Sr WO_4:Er^{3+}, Yb^{3+} composites were characterized by X-ray diffraction (XRD), scanning electron microscopy (SEM) and energy-dispersive X-ray spectroscopy (EDS). Spectroscopic properties have been investigated by photoluminescence emission measurements and Raman spectroscopy.

EXPERIMENTAL

Appropriate stoichiometric amounts of $SrCl_2·6H_2O$, $ErCl_3·6H_2O$, $YbCl_3·6H_2O$, $Na_2WO_4·2H_2O$, 5 nm sized Fe_3O_4 nanoparticles and ethylene glycol of analytic reagent grade were used to prepare the $SrWO_4$:Er^{3+}, Yb^{3+} and SPION/$SrWO_4$:Er^{3+}, Yb^{3+} compounds. To prepare $SrWO_4$:Er^{3+}/Yb^{3+}, 0.8 mol % $SrCl_2·6H_2O$ with 0.02 mol % $ErCl_3·6H_2O$ and 0.18 mol % $YbCl_3·6H_2O$ and 1 mol % $Na_2WO_4·2H_2O$ were dissolved in 30 mL of ethylene glycol. To prepare SPION/$SrWO_4$:Er^{3+}, Yb^{3+}, 0.2 mol % $SrCl_2·6H_2O$ with 0.02 mol % $ErCl_3·6H_2O$ and 0.18 mol % $YbCl_3·6H_2O$ and 1 mol % $Na_2WO_4·2H_2O$ with 0.5 mol % Fe_3O_4 were dissolved in 30 mL of ethylene glycol. The solutions were mixed and adjusted to pH 9.5 using NaOH. The solutions were stirred at room temperature. Then, the

mixtures were transferred into 120 mL Teflon vessels. Each Teflon vessel was placed into a microwave oven operating at the frequency of 2.45 GHz with the maximum output power of 1250 W for 23 min. The working cycle of the microwave-assisted metathetic reaction was been controlled very precisely between 30 sec on and 30 sec off for 8 min, followed by a further treatment of 30 sec on and 60 sec off for 15 min. Ethylene glycol was evaporated slowly at its boiling point. Ethylene glycol is a polar solvent at its boiling point of 197 °C and it is a good candidate for the microwave process. The resulted powder samples were treated with ultrasonic radiation and washed many times with hot distilled water. The white precipitates were collected and dried at 100 °C in a drying oven. After this, the final products were heat-treated at 600 °C for 3 h.

The phase composition of final powder products formed after the cyclic microwave-assisted metathetic reaction and following heat-treatment was identified using XRD (D/MAX 2200, Rigaku, Japan). The microstructures and surface morphologies of the $SrWO_4$:Er^{3+}/Yb^{3+} and SPION/$SrWO_4$:Er^{3+}/Yb^{3+} composites were observed using SEM/EDS (JSM-5600, JEOL, Japan). Their photoluminescence spectrum was recorded at room temperature using a spectrophotometer (Perkin Elmer LS55, UK). Raman spectroscopy measurements were performed using a LabRam HR (Jobin-Yvon, France) device. The 514.5-nm line of an Ar-ion laser was used as an excitation source and the power on the samples was kept at 0.5 mW.

RESULTS AND DISCUSSION

Fig. 1 shows the XRD patterns of (a) pure $SrWO_4$ (JCPDS: 08-0490) and (b) the synthesized SPION/$SrWO_4$:Er^{3+}/Yb^{3+} particles. All the diffraction peaks were assigned to the tetragonal-phase $SrWO_4$ with a Scheelite-type structure and Fe_3O_4, which were in good agreement with the crystallographic data of $SrWO_4$ (JCPDS: 08-0490) and Fe_3O_4 (JCPDS 19-0629). The diffraction peaks marked with asterisk are related to Fe_3O_4. The result confirms that the SPION/$SrWO_4$:Er^{3+}, Yb^{3+} composites can be prepared using the cyclic microwave-assisted metathetic route. The post-synthesis heat-treatment plays an important role in forming well-defined crystallized micromorphology. To achieve such morphology, the SPION/$SrWO_4$:Er^{3+}, Yb^{3+} composites need to be heated at 600 °C for 3 h. This

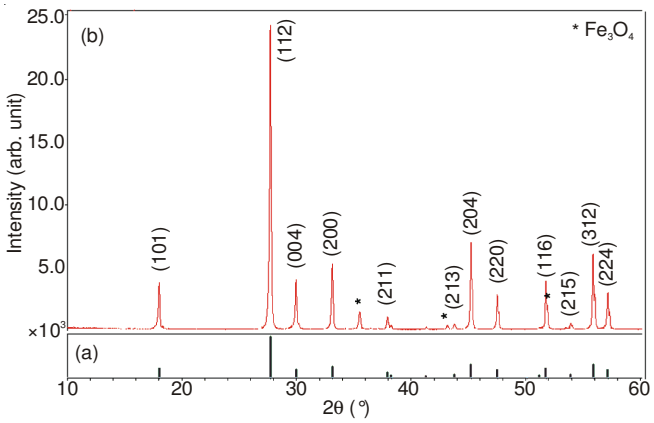

Fig. 1. XRD pattern of (a) pure $SrWO_4$ and (b) the synthesized SPION/$SrWO_4$:Er^{3+},Yb^{3+} composites

suggests that the cyclic microwave-assisted metathetic route, in combination with subsequent heat-treatment, is a suitable way for the formation of SPION/$SrWO_4$:Er^{3+}, Yb^{3+} polycrystalline composites with well developed high-intensity peaks from the at (112), (200) and (312) planes, which are the major peaks of $SrWO_4$[13-15].

The SEM image of the synthesized SPION/$SrWO_4$:Er^{3+}, Yb^{3+} composite is shown in Fig. 2. The as-synthesized sample has a well-defined and homogeneous morphology with the $SrWO_4$:Er^{3+}, Yb^{3+} particle size of 1-2 μm and Fe_3O_4 particle size of 0.1-0.5 μm, respectively. The Fe_3O_4 particles were self-preferentially crystallized and immobilized on the surface of $SrWO_4$:Er^{3+}, Yb^{3+} particles. The incorporation of Fe_3O_4 nanoparticles to the $SrWO_4$:Er^{3+}, Yb^{3+} compound particles can be successfully achieved using the cyclic microwave-assisted metathetic. The microwave-assisted metathetic reactions, such as $SrCl_2 + Na_2WO_4 \rightarrow SrWO_4 + 2NaCl$, involve the exchange of atomic/ionic species, in which the driving force is the exothermic reaction accompanying the formation of NaCl[16]. The SPION/$SrWO_4$:Er^{3+}, Yb^{3+} composites were heated rapidly and uniformly by the cyclic microwave-assisted metathetic route. This classifies the method among simple and cost-effective ones and, evidently, the microwave-assisted metathetic technology is able to provide high yields with an easy scale-up as a viable alternative for the rapid synthesis of complex oxide composites[17].

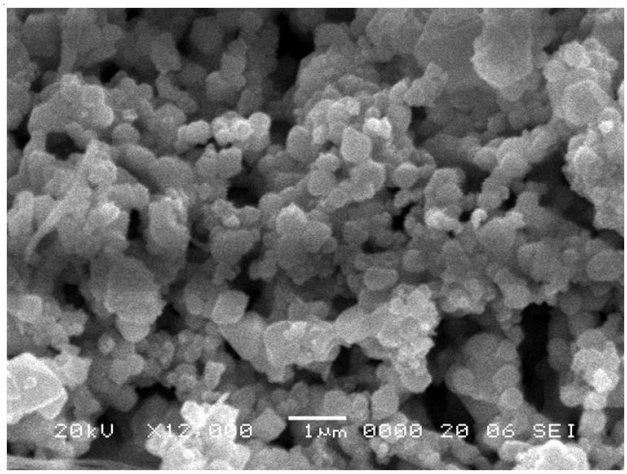

Fig. 2. A SEM image of the synthesized SPION/$SrWO_4$:Er^{3+}, Yb^{3+} composites

The recorded EDS pattern, quantitative compositions, quantitative results and the SEM image of the synthesized SPION/$SrWO_4$:Er^{3+}, Yb^{3+} composite are presented in Fig. 3. The EDS pattern shown in Fig. 3a displays that the SPION/$SrWO_4$:Er^{3+}, Yb^{3+} sample is composed of Fe, Sr, W, O, Er and Yb with the dominance of Fe, Sr, W, O. The EDS pattern and quantitative compositions in Fig. 3 a,b could be well assigned to the SPION/$SrWO_4$:Er^{3+}, Yb^{3+} composite. Thus, the incorporation of Fe_3O_4 nanoparticles to the SPION/$SrWO_4$:Er^{3+}, Yb^{3+} compound particles can be successfully achieved using the cyclic microwave-assisted metathetic. The cyclic microwave-assisted metathetic reactions provide a convenient route for the synthesis of such complex products as SPION/$SrWO_4$:Er^{3+}, Yb^{3+} composites. The cyclic microwave-assisted metathetic

(a)

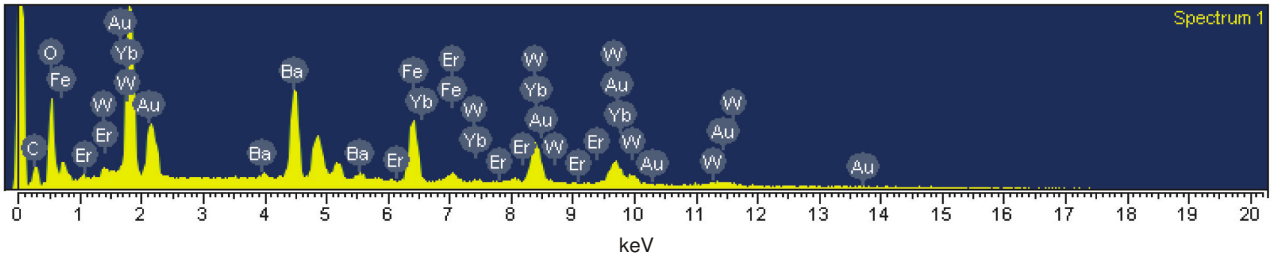

(b)

Spectrum	In stats.	C	O	Fe	Ba	Er	Yb	W	Au	Total
Spectrum 1	Yes	6.56	16.54	11.18	25.06	0.95	0.56	26.98	12.17	100.00
Mean		6.56	16.54	11.18	25.06	0.95	0.56	26.98	12.17	100.00
Std. deviation		0.00	0.00	0.00	0.00	0.00	0.00	0.00	0.00	
Max.		6.56	16.54	11.18	25.06	0.95	0.56	26.98	12.17	
Min.		6.56	16.54	11.18	25.06	0.95	0.56	26.98	12.17	

(c)

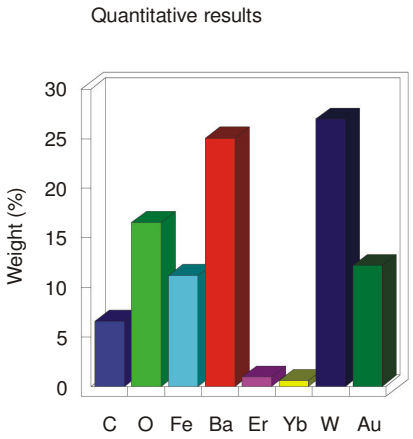

(d)

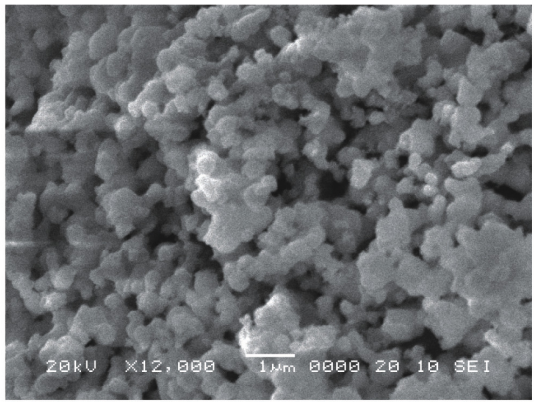

Fig. 3. (a) EDS pattern, (b) quantitative compositions, (c) quantitative results and (d) SEM image of the synthesized SPION/$SrWO_4$:Er^{3+}, Yb^{3+} composites

route provides the exothermic energy to synthesize the bulk of the material uniformly, so that fine particles with controlled morphology can be fabricated in an environmentally friendly manner and without solvent waste generation.

The photoluminescence emission spectra recorded from the synthesized SPION/$SrWO_4$:Er^{3+},Yb^{3+} composite excited at 250 nm at room temperature are shown in Fig. 4. It is generally assumed that the measured emission spectrum of metal tungstates are mainly attributed to the charge-transfer transitions within the $[WO_4]^{2-}$ complex[18,19]. With excitation at 250 nm, the spectra show rugged peaks, which are composed of three kinds of groups. The first major peaks are located at the blue wavelength 425-450 nm, the second neighbored shoulders at 460-490 and the third sloped shoulders at 530-550 nm. The emission spectra of 4-8 narrow neighbored and sloped shoulders, namely the spread-eagle-shape, at approximately 460-550 nm are considered to form by defect structures[20]. Generally, the presence of Gaussian components indicates that the electronic levels corresponding to relaxed excited state of of an emission centre belong to a degenerate excited state influenced by some perturbation, *e.g.* local low symmetry crystal field[21]. Such emission peaks can be explained by the influence of the Jahn-Teller effect[21,22] on the degenerated excited state of $[WO_4]^{2-}$ tetrahedron.

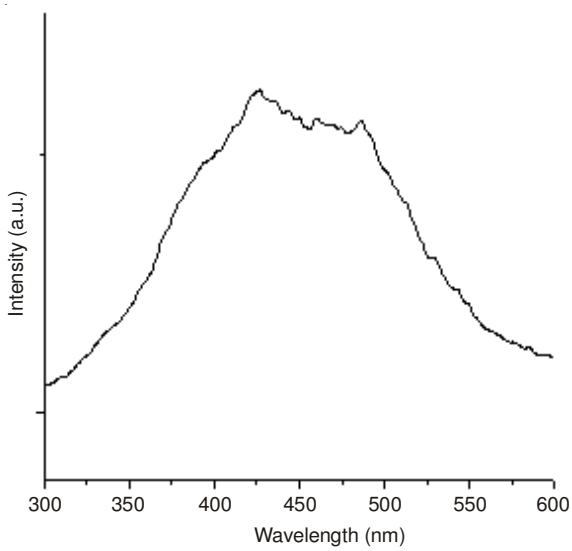

Fig. 4. Photoluminescence emission spectrum of the synthesized SPION/$SrWO_4$:Er^{3+}, Yb^{3+} composite excited at 250 nm at room temperature

Fig. 5 shows the Raman spectra of the synthesized (a) $SrWO_4$ particles and (b) $SrWO_4$: Er^{3+}, Yb^{3+} (SWO:ErYb) and SPION/$SrWO_4$:Er^{3+}, Yb^{3+} (F-SWO:ErYb) composites excited by the 514.5-nm line of an Ar-ion laser at 0.5 mW. The Raman

modes for the $SrWO_4$ particles in Fig. 5a were detected as $\nu_1(A_g)$, $\nu_3(B_g)$, $\nu_3(E_g)$, $\nu_4(E_g)$, $\nu_4(Bg)$ and $\nu_2(Bg)$ vibrations at 920, 836, 798, 371, 334 and 235 cm^{-1}, respectively. A free rotation mode was detected at 187 cm^{-1} and external modes were localized at 133 cm^{-1}. The well-resolved sharp peaks for the $SrWO_4$ particles provide that the synthesized particles are highly crystallized. The vibration modes in the Raman spectrum of tungstates are classified into two groups, internal and external[23,24] internal vibrations are related to the $[WO_4]^{2-}$ molecular group with a stationary mass center. The external vibrations or lattice phonons are associated to the motion of the Sr^{2+} cation and rigid molecular units. The type of cations (Ca^{2+}, Sr^{2+}, Ba^{2+}) can influence on the Raman modes by changing the size of the crystal unit cell and by covalent cation effect[24]. The essential dependence of the bandwidth on the peculiarities of crystal lattice and the type of M^{2+} cation in the series of MWO_4 (M = Ca, Sr, Ba, Pb) crystals with Scheelite structure. The moving in the series of tungstates $Ca^2 \rightarrow Sr^{2+} \rightarrow Ba^{2+}$ increases the unit cell and interionic distance inside the molecular group. The degree of covalent bond between the cation and molecular group usually decreases within the series $Ca^2 \rightarrow Sr^{2+} \rightarrow Ba^{2+}$. This anomalous phenomenon can be explained by decreasing of interaction between internal and external Raman modes in the scheelite structure in metal tungstates.

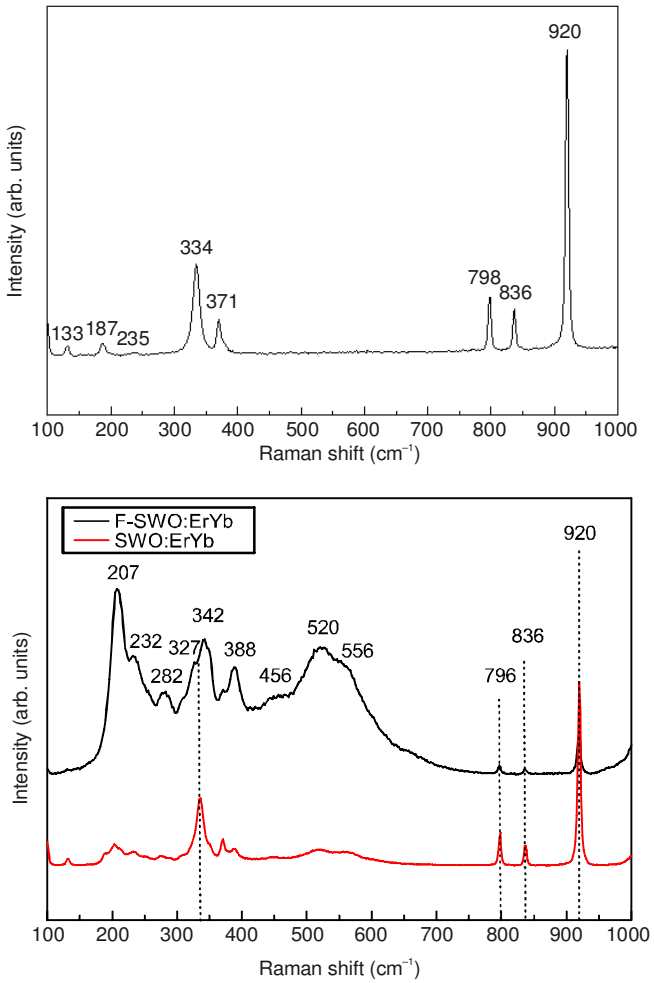

Fig. 5. Raman spectra of the synthesized (a) $SrWO_4$ particles and (b) $SrWO_4$:Er^{3+}, Yb^{3+} (SWO:ErYb) and SPION/$SrWO_4$:Er^{3+}, Yb^{3+} (F-SWO: ErYb) composites

The internal modes for the $SrWO_4$:Er^{3+}, Yb^{3+} (SWO:ErYb) and SPION/$SrWO_4$:Er^{3+}, Yb^{3+} (F-SWO:ErYb) composites in Fig. 5b were detected as $\nu_1(A_g)$, $\nu_3(B_g)$, $\nu_3(E_g)$, $\nu_4(E_g)$, $\nu_4(B_g)$ and $\nu_2(B_g)$ vibrations at 920, 836, 796, 388, 342 and 232 cm^{-1}, respectively. The external modes were localized at 207-115 cm^{-1}. From the comparison in Fig. 5b it can be depicted that the peak positions are practically the same, while the intensities obtained from $SrWO_4$:Er^{3+}, Yb^{3+} (SWO:ErYb) are slightly higher than those of SPION/$SrWO_4$:Er^{3+}, Yb^{3+} (F-SWO:ErYb). The internal vibration mode frequencies are dependent on the lattice parameters and the degree of the partially covalent bonding between the cations and molecular ionic group $[WO_4]^{2-}$[24]. The Raman spectra of the synthesized $SrWO_4$:Er^{3+}, Yb^{3+} (SWO:ErYb) and SPION/$SrWO_4$:Er^{3+}, Yb^{3+} (F-SWO:ErYb) composites indicate additional peaks at both middle (556, 520 and 456 cm^{-1}) and lower frequencies (327 and 282 cm^{-1}), which are attributed to the doping ions of Er^{3+} and Yb^{3+}[25-28]. It is noted that the Fe_3O_4 particles have no influence on the Raman spectra, while the doping ion of Er^{3+}/Yb^{3+} can influence the Raman spectra. The Raman spectra proved that the Er^{3+}/Yb^{3+} doping ions can influence the structure of the host materials.

Conclusion

The SPION/$SrWO_4$:Er^{3+}, Yb^{3+} composites were successfully synthesized by the cyclic microwave-assisted metathetic method. The microstructure exhibited a well-defined and homogeneous morphology with the $SrWO_4$: Er^{3+}, Yb^{3+} and Fe_3O_4 particle size of 1-2 and 0.1-0.5 μm, respectively. The Fe_3O_4 nanoparticles were self-preferentially crystallized and immobilized on the surface of $SrWO_4$: Er^{3+}, Yb^{3+} particles. The Raman spectra of the synthesized $SrWO_4$: Er^{3+}, Yb^{3+} (SWO: ErYb) and SPION/$SrWO_4$: Er^{3+}, Yb^{3+} (F-SWO: ErYb) composites indicate additional peaks at both middle (556, 520 and 456 cm^{-1}) and lower frequencies (327 and 282 cm^{-1}), which are attributed to the doping ions of Er^{3+} and Yb^{3+}.

ACKNOWLEDGEMENTS

This study was supported by Basic Science Research Program through the National Research Foundation of Korea (NRF) funded by the Ministry of Education, Science and Technology (2013-054508).

REFERENCES

1. D. Liu, L. Tong, J. Shi and H. Yang, *J. Alloys Comp.*, **512**, 361 (2012).
2. L. Liu, L. Xiao and H.Y. Zhu, *Chem. Phys. Lett.*, **539-540**, 112 (2012).
3. Q. Wang, X. Yang, L. Yu and H. Yang, *J. Alloys Comp.*, **509**, 9098 (2011).
4. Z. Shan, Y. Wang, H. Ding and F. Huang, *J. Mol. Catal. A*, **302**, 54 (2009).
5. H. Wu, Y. Hu, F. Kang, L. Chen, X. Wang, G. Ju and Z. Mu, *Mater. Res. Bull.*, **46**, 2489 (2011).
6. G.H. Lee and S. Kang, *J. Lumin.*, **131**, 2606 (2011).
7. F.B. Cao, L.S. Li, Y.W. Tian, Y.J. Chen and X.R. Wu, *Thin Solid Films*, **519**, 7971 (2011).
8. J. Liao, B. Qiu, H. Wen, J. Chen, W. You and L. Liu, *J. Alloys Comp.*, **487**, 758 (2009).
9. Y. Zheng, Y. Huang, M. Yang, N. Guo, H. Qiao, Y. Jia and H. You, *J. Lumin.*, **132**, 362 (2012).
10. M. Sadegh, A. Badiei, A. Abbasi, H. Goldooz and G. Mohammadi Ziarani, *J. Lumin.*, **130**, 2072 (2010).
11. W. Wang, P. Yang, S. Gai, N. Niu, F. He and J. Lin, *J. Nanopart. Res.*, 12, 2295 (2010).

12. Y. Tian, Y. Liu, R. Hua, L. Na and B. Chen, *Mater. Res. Bull*., **47**, 59 (2012).
13. R. Dinesh, T. Fujiwara, T. Watanabe, K. Byrappa and M. Yoshimura, *J. Mater. Sci*., **41**, 1541 (2006).
14. D. Rangappa, T. Fujiwara, T. Watanabe and M. Yoshimura, *J. Electroceram*., **17**, 853 (2006).
15. T. Thongtem, A. Phuruangrat and S. Thongtem, *J. Nanopart. Res*., **12**, 2287 (2010).
16. C.S. Lim, *Mater. Chem. Phys*., **131**, 714 (2012).
17. C.S. Lim, *J. Lumin*., **132**, 1774 (2012).
18. D.A. Spassky, S.N. Ivanov, V.N. Kolobanov, V.V. Mikhailin, V.N. Zemskov, B.I. Zadneprovski and L.I. Potkin, *Radiat. Measur*., **38**, 607 (2004).
19. G.Y. Hong, B.S. Jeon, Y.K. Yoo and J.S. Yoo, *J. Electrochem. Soc*., **148**, H161 (2001).
20. M. Nikl, P. Bohacek, E. Mihokova, M. Kobayashi, M. Ishii, Y. Usuki, V. Babin, A. Stolovich, S. Zazubovich and M. Bacci, *J. Lumin*., **87-89**, 1136 (2000).
21. K. Polak, M. Nikl, K. Nitsch, M. Kobayashi, M. Ishii, Y. Usuki and O. Jarolimek, *J. Lumin*., **72-74**, 781 (1997).
22. F.S. Ham, *J. Lumin*., **85**, 193 (2000).
23. T.T. Basiev, A.A. Sobol, Y.K. Voronko and P.G. Zverev, *Opt. Mater.*, **15**, 205 (2000).
24. T.T. Basiev, A.A. Sobol, P.G. Zverev, L.I. Ivleva, V.V. Osiko and R.C. Powell, *Opt. Mater*., **11**, 307 (1999).
25. C.S. Lim, *Mater. Res. Bull*., **47**, 4220 (2012).
26. V.V. Atuchin, V.G. Grossman, S.V. Adichtchev, N.V. Surovtsev, T.A. Gavrilova and B.G. Bazarov, *Opt. Mater*., **34**, 812 (2012).
27. C.S. Lim, *Mater. Res. Bull*., **48**, 3805 (2013).
28. C.S. Lim, *Mater. Chem. Phys*., **140**, 154 (2013).